

COMPRESSIVE STRENGTH OF PLA BASED SCAFFOLDS: EFFECT OF LAYER HEIGHT, INFILL DENSITY AND PRINT SPEED

Harshit K. Dave, Shilpesh R. Rajpurohit, Naushil H. Patadiya, Shalin J. Dave, Kumar S. Sharma, Siddharth S. Thambad, Varunkumar P. Srinivasn, Khyati V. Sheth

Department of Mechanical Engineering, Sardar Vallabhbhai National Institute of Technology, Surat-395 007, India

Corresponding author: Harshit K. Dave, harshitkumar@yahoo.com

Abstract: In the field of tissue engineering, the scaffold is required to provide a suitable environment for tissue regeneration. The scaffold should have desired mechanical properties that mimic the properties of the tissue. Fused deposition modeling (FDM) is one of the most widely used additive manufacturing process that can be used for scaffold fabrication. The mechanical properties of the fabricated scaffold are greatly dependent on the printing parameters. The goal of this study to evaluate the influence of the print parameter on the mechanical properties of the printed scaffold. Hence, in the present study three important process parameter namely, layer height, infill density, and print speed have been selected to study their effect on the mechanical strength by performing a compressive test. The scaffold has been fabricated using biocompatible, biodegradable Poly-lactic acid (PLA) material and compression test perform in accordance with ASTM D695 standard. Results reveal that compressive strength is significantly affected by infill density. Higher compressive strength was obtained at the higher infill density with a low porous structure. Suitable infill density has to be applied so that scaffold can be obtained with required porosity and compressive strength.

Key words: fused deposition modelling, poly-lactide acid (PLA), layer height, infill density, compressive strength

1. INTRODUCTION

Tissue engineering is combination cells, engineering and material method to improve or replace tissue function. Tissue engineering involves the application of scaffold for the regeneration or formation of cells or tissues. The scaffold must be 3D dimensional, highly interconnected porous and have sufficient porosity for cell growth. It is important to produce a scaffold with desired mechanical properties that mimic the properties of the tissue in the immediate vicinity of the defect. Many traditional processing techniques have been used to manufacture 3D dimensional scaffold for tissue engineering applications. The constraint associated with existing techniques encouraged the use of additive manufacturing (AM) techniques for scaffold

fabrication (Sultana, 2018).

For tissue engineering, AM allows the 3D printing of various scaffold design for a specific patient requirement. FDM is one of the most popular AM technique that can be effectively used to print the scaffolds for tissue engineering application. FDM is allowing one to fabricate parts containing complex internal and external structures with relatively good accuracy using thermoplastic material. It also has the added advantage of being simple in principle, in terms of the mechanisms and the cheap and ready availability of printing materials. Due to these advantages, it has been a widely accepted AM technique for the fabrication of part in various industries such as aviation, medical, automobile etc. The mechanical properties of the scaffold are very crucial. For the tissue engineering application, the scaffold must simulate the mechanical properties of the tissue to be replaced. Since the mechanical properties of the scaffold are closely related to the porosity of the scaffold, it might be stiffer and less porous scaffold will provide better integration with surrounding with natural tissue and less porous scaffold will provide a cell for better attachment and reproduction. FDM offers opportunities to meet the different requirement in one scaffold (Korpela et al., 2013; Moroni et al., 2006).

Ang et al. (2006) examined the impact of build variables on the porosity and compressive strength of FDM fabricated ABS scaffold. They reported that the air gap and raster width is the most significant process parameter that affects the porosity and compressive strength of ABS scaffold. Cerreti et al. (2017) explore the influence of two different extrusion technology (filament extrusion and grain extrusion) on the dimensional accuracy of the FDM produced scaffold. The pore size of the scaffold is more stable and uniform when using the filament extrusion method. Chim et al. (2006) studied the compressive strength of the FDM manufactured scaffold using PCL, PCL/HA, and PCL/SBF material. They observed that Scaffold fabricated using PCL have better compressive properties over the PCL/HA and PCL/SBF. Weiding et

al. (2012) examined the influence of structure shape and strut orientation on the compressive strength of additively manufactured titanium scaffold. Scaffold fabricated with rectangular strut aligned in vertical direction displayed better compressive properties. Guan et al. (2004) investigated the mechanical strength for poly(lactide-co-glycolide) (PLGA)/calcium phosphate (CaP) scaffold for bone tissue engineering application. They observed 31.6% more dry compressive strength over to wet compressive strength. They also reported that higher the Cap/PLGA ratio improve the mechanical properties. Hutmacher et al. (2001) performed the experimental study on the influence of laydown pattern on the mechanical strength of the FDM produced PCL scaffold. They obtained the higher compressive strength for a scaffold with 0°/60°/120° laydown patterns over 0°/72°/144°/36°/108° laydown patterns. Mishra et al. (2017) studied the impact of build variables on the compressive strength of the FDM part. They reported that built orientation, number of counters and air gap has a significant effect on the compressive strength of the part. Hernandez et al. (2016) reported the impact of build orientation on the compressive strength of the FDM produced part. Parts printed in a XY plan have higher compressive strength over Z-plane. Motapatri et al. (2016) reported the impact of build orientation, raster angle and air gap on the compressive strength of FDM processed ABS. They reported that horizontally build specimen have higher compressive strength over the vertically build specimen. Sood et al. (2012) reported the impact of build parameter on the compressive strength of FDM produced ABS part. Compressive strength is found to be decreased with a lower value of layer thickness and a higher air gap. Upadhyay et al. (2017) reported that perpendicularly deposited layer help achieve a higher compressive strength. Ahn et al. (2002) observed that horizontally build specimen have higher compressive strength over transversely build specimen. Jami et al. (2018) reported that a solid build specimen have higher compressive strength over sparse build specimen. Zein et al. (2002) used FDM techniques to fabricate the PCL scaffolds. They observed that the mechanical strength of scaffold is mostly dependent on the porosity irrespective of laydown pattern. Murugan et al. (2018) investigated the effect of build variables on the mechanical behavior of FDM based 3D printed part. They observed that layer thickness significantly affecting ultimate tensile strength and print time while extrusion temperature significantly affecting elastic modulus.

The literature reveals that FDM has been used to print the scaffold for tissue engineering applications. The scaffold must have sufficient mechanical strength with appropriate porosity for effective functioning in tissue engineering. The mechanical strength of the scaffold is greatly dependent on the selection of print parameters. The aim of this study to determine the

effect of print parameters on the mechanical strength of FDM printed scaffold.

2. MATERIALS AND METHOD

In the present investigation, PLA material has been used to fabricate the porous scaffold. Table 1 shows the properties of the PLA material used in the present study. Using PLA material all the scaffold test samples were printed using Prusa plus 3D printer, a high precision (position accuracy = 11µm, nozzle diameter = 0.4 mm) open architect 3D printed based on fused deposition modeling process. Initially, the scaffold was design in Autodesk Inventor and save as STL file. STL file is then imported into the slicing software wherein all the process parameters have been adjusted to fabricate the scaffold, then after STL file was sliced. Finally, a gcode file that contained the printing instruction was generated and transferred to the 3D printer.

Table 1. Material Properties of PLA

Properties	Units	Value
Melting Point	°C	190-220
Density	g/cm ³	1.20-1.25
Diameter of Filament	mm	1.75
Tensile Yield Strength	MPa	62.63
Elongation at Break	%	4.43
Flexural Strength	MPa	65.02
Flexural Modulus	MPa	2504.4
Impact Strength	KJ/m ²	4.28

Among the various 3D printing parameters, three printing parameters namely, layer thickness, infill density, and print speed has been selected to study their influence on the compressive strength of the printed scaffold. As the aim of the present investigation, to study the compressive strength of the printed scaffold, scaffold test samples are designed and fabricated as per the ASTM D695, which specifies the geometry and dimensions of the test sample. As indicated in Figure 1 shows the schematic diagram of the designed compression specimen to be fabricated at the different printing parameters.

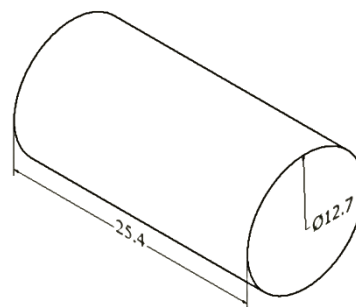


Fig. 1. Compression test specimen according to ASTM D695 (all dimensions are in mm)

Layer height is the thickness of each layer deposited during the part printing. Three layer height has been selected and varied as 0.1mm, 0.2mm and 0.3mm as per the capacity of the built printer. Infill density defines the amount of material required inside print. Higher infill density leads to more material and smaller pore size while smaller infill density leads to less material and bigger pore size inside. Three different infill density has been selected and varied at 60%, 70%, and 80%. Print speed is the speed of the deposition of the material to fabricate the specimen. Three different print speed has been considered and varied at 30mm/min, 40mm/min and 50mm/min. For all three printing variables and their corresponding three levels as shown in Table 2, total of 27 experiments need to be performed as per the full factorial experimental design. All the experiments have been performed three times to ensure the repeatability of the results, which results in a total 81 experimental runs. During the printing of scaffold, PLA material is extruded at 210°C while the bed temperature kept at 70°C and the raster width keep constant at 0.4mm.

Table 2. Value of the Input Parameters

Parameters	Unit	Level 1	Level 2	Level 3
Layer height (h_L)	mm	0.1	0.2	0.3
Infill density (ρ_d)	%	60	70	80
Print speed (S_P)	mm/min	30	40	50

Scaffolds were printed according to the geometry and outer dimension defined in ASTM D695-Standard Test Method for Compressive Properties of Rigid Plastics (as shown in Figure 1). All the compressive tests were performed using electronic tensometer (PC2000, Kudale Instruments Pvt. Ltd.). For each sample, compression plates were initially set 25.4mm apart from each other and compression was continuing at 1.3mm/min until maximum compression load was achieved. Load and displacement data were recorded using a software program for further analysis.

3. RESULT AND DISCUSSION

All the scaffold test specimens have been fabricated and tested according to ASTM D695 standard as derived by full factorial experimental design. Table 3 shows the mean compressive strength and the S/N ratio for each experimental run.

The graphs of the mean values of S/N ratios have been plotted for each process parameters are shown in Figure 2. It is desirable to a have higher compressive strength, so the main effect plot has been construed using the “larger-the-better” characteristics. The analysis of the S/N ratio reveals that the optimal performance of the strength is obtained at a layer height of 0.2mm, an infill density of 80% and a print speed of 40mm/min.

Table 3. Experimental results obtained through a compression test

Layer Height (mm)	Infill Density (%)	Print Speed (mm/min)	Mean Compressive Strength (N/mm ²)	S/N Ratio
0.1	60	30	31.790	30.042
		40	31.973	30.092
		50	29.540	29.364
	70	30	34.847	30.722
		40	38.490	31.668
		50	36.137	31.033
	80	30	52.983	34.479
		40	52.477	34.353
		50	52.577	34.379
0.2	60	30	30.960	30.960
		40	33.543	33.543
		50	31.073	31.073
	70	30	42.480	42.480
		40	43.120	43.120
		50	43.617	43.617
	80	30	52.593	52.593
		40	52.927	52.927
		50	33.130	39.243
0.3	60	30	26.460	26.460
		40	30.060	30.060
		50	26.673	26.673
	70	30	39.437	39.437
		40	37.913	37.913
		50	37.520	37.520
	80	30	50.773	50.773
		40	49.730	49.730
		50	52.153	52.153

It can also be seen that compression strength is greatly affected by the infill density. Compression strength is found to be increased with increment in infill density. While layer height and print speed does not show any specific effect on compressive strength.

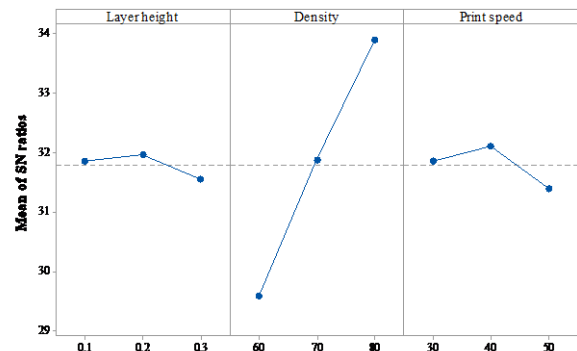


Fig. 2. Main effect of process variables on compressive strength

Further, Analysis of variance has been carried out to find out the process variables that significantly affect the compressive strength of the printed scaffold. Table 4 shows the analysis of variance carried out to identify the significant process variables affecting compression strength. From ANOVA analysis, it can be observed that infill density is only a significant process variable affecting the compressive strength of test specimen with 87.07 % contribution.

Table 4. Analysis of Variance for compressive strength

Factor	DOF	SS	Adj MS	F-Value	P-Value
Layer Height	2	19.75	9.873	0.85	0.442
Infill Density	2	1876.02	938.008	80.82	0.000
Print Speed	2	26.80	13.400	1.15	0.335
Error	20	232.13	11.606		
Total	26	2154.69			

3.1. Effect of layer height

Figures 3(a-c) shows the variation of the compressive strength of the test specimens with respect to layer heights while keeping the print speed constant and varying the infill density. It can be observed that compressive strength is found to be increased with increment in layer height up to 0.2 mm then its start decreasing. In most of the cases, higher compressive strength has been observed with 0.2 mm layer height except in the case of the sample printed at 50 mm/min having an 80% infill density and a layer height of 0.2 mm is observed.

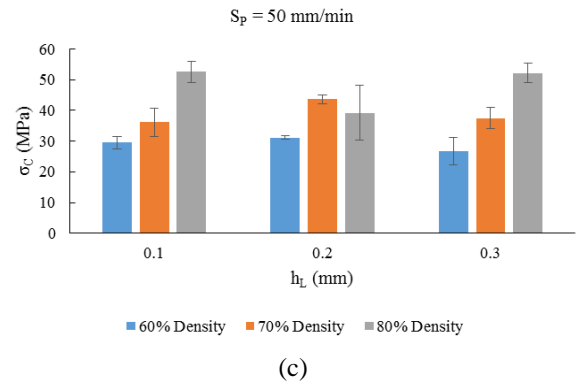
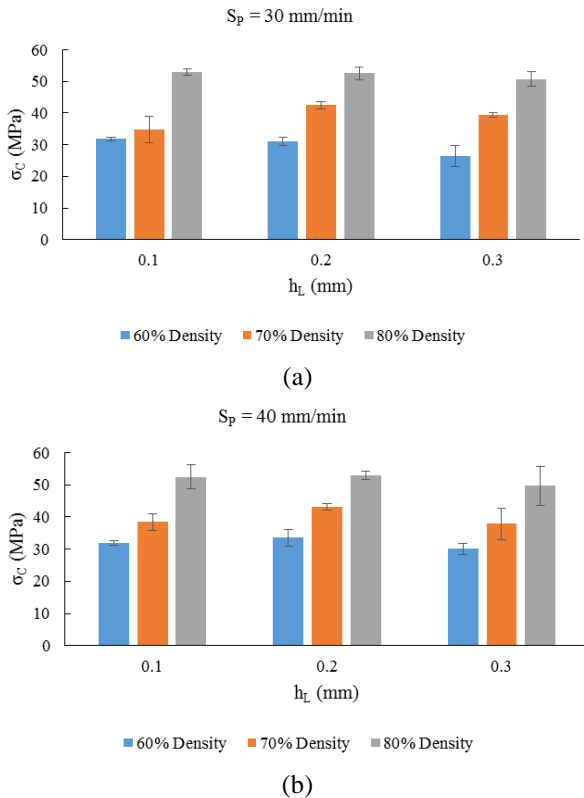


Fig. 3. Effect of layer height on compressive strength with different infill density at (a) 30 mm/min, (b) 40 mm/min and (c) 50 mm/min printing speed

It is observed that an increase in strength of almost 15% from layer height of 0.1mm to 0.3mm for 70% infill density and an increase of about 20% from 0.1mm to 0.2 mm is observed. At lower layer height, more bonding line appeared in the part due to more numbers of a layer. There is more chance of layer displacement as interface bonding between layers is comparatively weaker than the monofilament that results in lower strength. Figure 4 shows the test specimen after the compression test wherein bulging can be observed with the tested specimen.

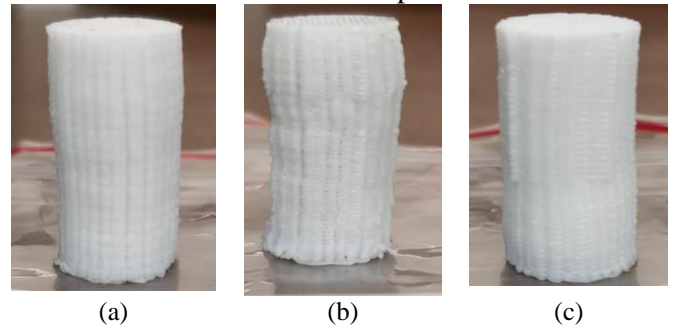


Fig. 4. Specimens after compression testing at (a) 0.1 mm, (b) 0.2 mm and (c) 0.3 mm layer height

3.2. Effect of infill density

Figures 5(a-c) shows the variation of the compressive strength of the test specimens with respect to infill density while keeping the layer height constant and varying the print speed. It can be observed that the compressive strength of the specimen is found to be increasing with increment in the infill density. It may be due to that at higher infill density larger amount of material is consumed to print the part due to a smaller opening in each cell. More amount of material tends to improve the strength of the printed part. Figure 6 shows the microscopic images of the test specimen at different infill density. Larger pores size can be observed with the 60% infill density, while smaller pore size can be observed for 80% infill density. Smaller pore size structure may have more material that can

withstand the higher loading during testing, which results in higher compressive strength. The porosity is an important element from the medical point of view to allow cell proliferation for medical applications. It is noticeable that as the density increases the size of the pore decreases and thereby enhancing mechanical properties.

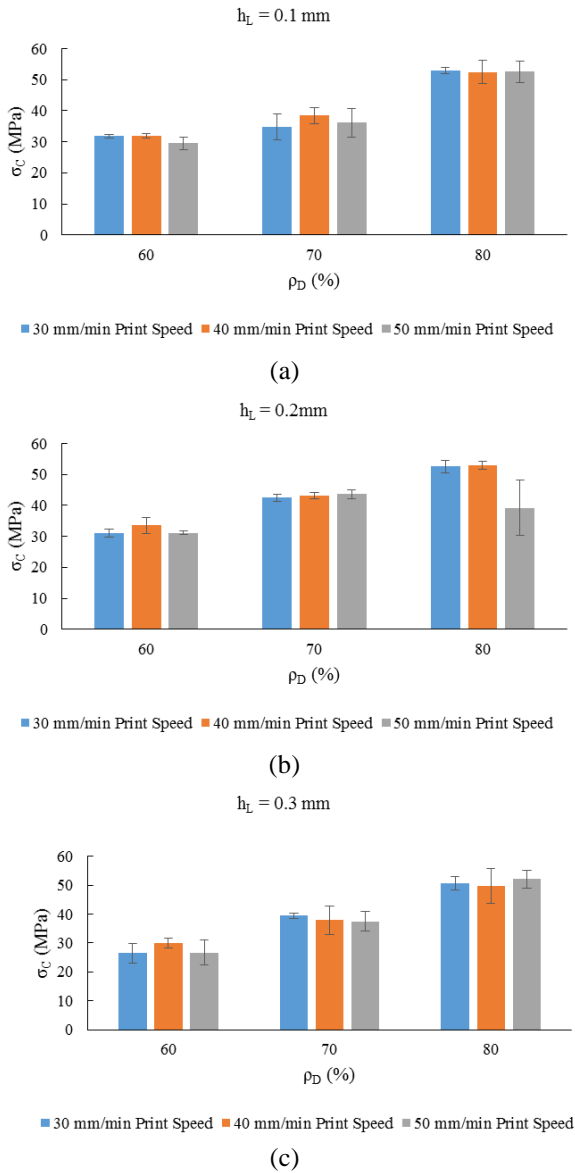


Fig. 5. Effect of infill density on compressive strength with different print speed at (a) 0.1 mm, (b) 0.2 mm and (c) 0.3 mm layer height

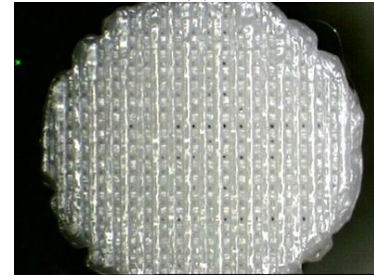
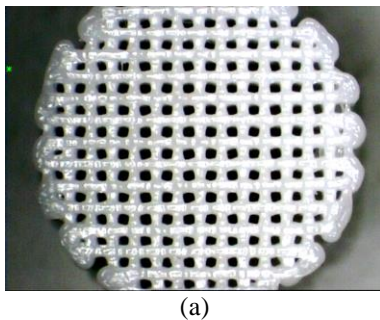
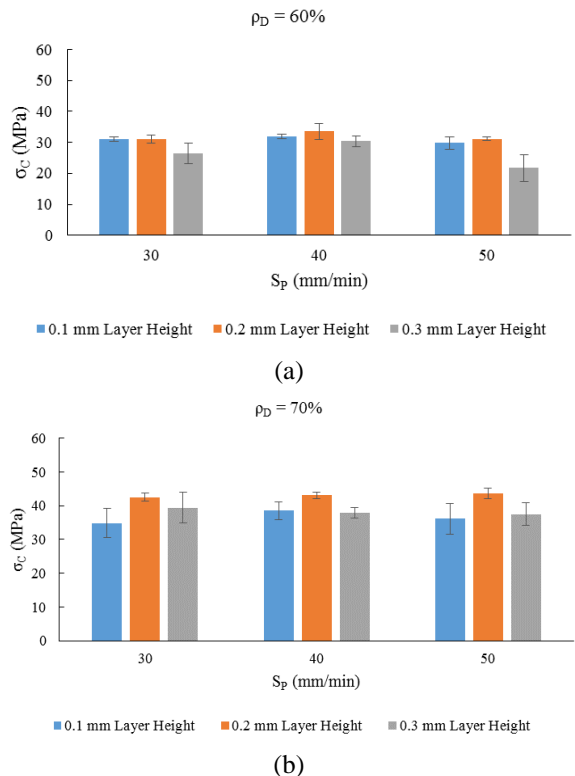


Fig. 6. Microscopic images of test specimen with different infill density (a) 60 %, (b) 70% and (c) 80%

3.3. Effect of print speed

Figures 7(a-c) shows the variation of the compressive strength of the test specimens with respect to print speed while keeping the infill density constant and varying the layer height. It is visible from Figure 7 that the variation in the compressive strength along with the print speed is very slight, however, it is also observed that the strength increases from an initial value till 40mm/min after which strength is found to be decreasing. This trend until a print speed of 40mm/min is observed in all the three layer heights. ANOVA analysis also confirms that print speed does not have any significant effect on the compressive strength.



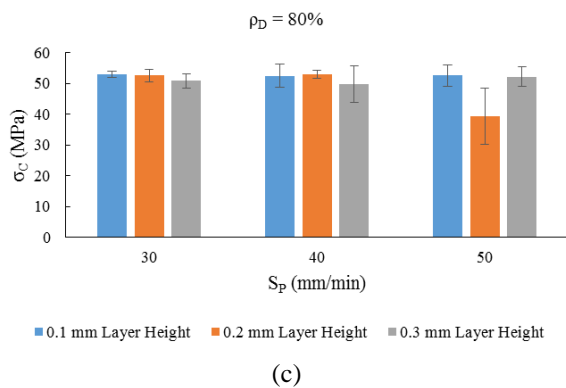


Fig. 7. Effect of print speed on compressive strength with different layer height at (a) 60%, (b) 70% and (c) 80% infill density

4. CONCLUSIONS

Experimental investigation on the effect of process variables viz. layer height, infill density and print speed on the compressive strength of the 3D printed PLA based scaffolds has been carried out according to the ASTM D695 standard. Following are the main conclusions can be drawn from the present study.

The analysis of the S/N ratio reveals that the optimal performance of the strength is obtained at a layer height of 0.2 mm, an infill density of 80% and a print speed of 40 mm/min.

Infill density found to be the most significant process parameter that affects the compressive strength of the printed part.

Layer height and print speed does not have any significant effect of the compressive strength of the test specimen.

Porosity can be controlled by controlling the infill density of the printed size. The porosity is an important element from the medical point of view to allow cell proliferation for medical applications.

5. REFERENCES

- Sultana, N., (2018). *Mechanical and biological properties of scaffold materials*. In Functional 3D Tissue Engineering Scaffolds, Deng, Y, Kuipe, J,(eds), 1-21.
- Korpela, J., Kokkari, A., Korhonen, H., Malin, M., Närhi, T., Seppälä, J., (2013). *Biodegradable and bioactive porous scaffold structures prepared using fused deposition modeling*, Journal of Biomedical Materials Research Part B: Applied Biomaterials, 101(4), 610-619.
- Moroni, L., De Wijn, J.R., Van Blitterswijk, C.A., (2006). *3D fiber-deposited scaffolds for tissue engineering: influence of pores geometry and architecture on dynamic mechanical properties*, Biomaterials, 27(7), 974-985.
- Chin Ang, K., Fai Leong, K., Kai Chua, C., Chandrasekaran, M., (2006). *Investigation of the*

mechanical properties and porosity relationships in fused deposition modelling-fabricated porous structures, Rapid Prototyping Journal, 12(2), 100-105.

5. Ceretti, E., Ginestra, P., Neto, P.I., Fiorentino, A., Da Silva, J.V.L., (2017). *Multi-layered scaffolds production via Fused Deposition Modeling (FDM) using an open source 3D printer: process parameters optimization for dimensional accuracy and design reproducibility*, Procedia CIRP, 65, 13-18.

6. Chim, H., Hutmacher, D.W., Chou, A.M., Oliveira, A.L., Reis, R.L., Lim, T.C., Schantz, J.T., (2006). *A comparative analysis of scaffold material modifications for load-bearing applications in bone tissue engineering*, International journal of oral and maxillofacial surgery, 35(10), 928-934.

7. Wieding, J., Jonitz, A., Bader, R., (2012). *The effect of structural design on mechanical properties and cellular response of additive manufactured titanium scaffolds*, Materials, 5(8), 1336-1347.

8. Guan, L., Davies, J.E., (2004). *Preparation and characterization of a highly macroporous biodegradable composite tissue engineering scaffold*, Journal of Biomedical Materials Research Part A: An Official Journal of The Society for Biomaterials, The Japanese Society for Biomaterials, and The Australian Society for Biomaterials and the Korean Society for Biomaterials, 71(3), 480-487.

9. Hutmacher, D.W., Schantz, T., Zein, I., Ng, K.W., Teoh, S.H., Tan, K.C., (2001). *Mechanical properties and cell cultural response of polycaprolactone scaffolds designed and fabricated via fused deposition modeling*, Journal of Biomedical Materials Research: An Official Journal of The Society for Biomaterials, The Japanese Society for Biomaterials, and The Australian Society for Biomaterials and the Korean Society for Biomaterials, 55(2), 203-216.

10. Mishra, S.B., Abhishek, K., Satapathy, M.P., Mahapatra, S.S., (2017). *Parametric Appraisal of Compressive Strength of FDM Build Parts*, Materials Today: Proceedings, 4(9), 9456-9460.

11. Hernandez, R., Slaughter, D., Whaley, D., Tate, J., Asiabanpour, B., (2016). *Analyzing the tensile, compressive, and flexural properties of 3D printed ABS P430 plastic based on printing orientation using fused deposition modeling*, In 27th Annual International Solid Freeform Fabrication Symposium, Austin, TX, pp. 939-950.

12. Motaparti, K.P., Taylor, G., Leu, M.C., Chandrashekhara, K., Castle, J., Matlack, M., (2016). *Effects of build parameters on compression properties for ULTEM 9085 parts by fused deposition modeling*, In Proceedings of the 27th Annual International Solid Freeform Fabrication Symposium, Austin, TX, USA, pp. 8-10.

13. Sood, A.K., Ohdar, R.K., Mahapatra, S.S., (2012). *Experimental investigation and empirical*

modelling of FDM process for compressive strength improvement, Journal of Advanced Research, 3(1), 81-90.

14. Upadhyay, K., Dwivedi, R., Singh, A.K., (2017). *Determination and comparison of the anisotropic strengths of fused deposition modeling P400 ABS*, In Advances in 3D Printing & Additive Manufacturing Technologies, Wimpenny, D.I., Pandey, P.M., Kumar, L.J., (Eds.) pp. 9-28, Springer, Singapore.

15. Ahn, S.H., Montero, M., Odell, D., Roundy, S., Wright, P.K., (2002). *Anisotropic material properties of fused deposition modeling ABS*, Rapid prototyping journal, 8(4), 248-257.

16. Jami, H., Masood, S.H., Song, W.Q., (2018). *Dynamic stress-strain compressive behaviour of FDM made ABS and PC parts under high strain rates*, In IOP Conference Series: Materials Science and Engineering, 377(1), 012153.

17. Zein, I., Hutmacher, D.W., Tan, K.C., Teoh, S.H., (2002). *Fused deposition modeling of novel scaffold architectures for tissue engineering applications*, Biomaterials, 23(4), 1169-1185.

18. Murugan, R., Mitilesh, R.N., Singamneni, S., (2018). *Influence of process parameters on the mechanical behaviour and processing time of 3D printing*, International Journal of Modern Manufacturing Technologies, 10(1), 69-75.

Received: January 15, 2019 / Accepted: June 15, 2019 / Paper available online: June 20, 2019 © International Journal of Modern Manufacturing Technologies.